An experimental and theoretical study of the photoemission from Ni(110)

1991 J. Phys.: Condens. Matter 3 1337

(http://iopscience.iop.org/0953-8984/3/10/011)

J. Phys.: Condens. Matter 3 (1991) 1337–1350. Printed in the UK

An experimental and theoretical study of the photoemission from Ni(110)

M A Hoyland† and R G Jordan†‡

Alloy Research Center, Department of Physics, Florida Atlantic University, Boca Raton, FL 33431-0991, USA

Received 3 August 1990

Abstract. We have investigated the electronic structure of the d bands in Ni along the $\Gamma(\Sigma)K(S)X$ direction using a combination of angle-resolved UV photoemission measurements and photocurrent calculations including correlation effects. In the calculations we used a potential for the excited state that included self-energy corrections based on the model of Tréglia *et al*. The calculations reproduce all of the main features in the experimental spectra. In particular, there is good agreement with the observed dispersion of the quasiparticle states of $\Sigma_3(S_3)$ and $\Sigma_4(S_4)$ symmetry. The calculations indicate that the correlations produce a marked energy dependence of the exchange splitting, in contrast to the essentially rigid shift obtained in standard one-electron calculations, and the results for the $\Sigma_4^{\uparrow\downarrow}$ states are in very good agreement with photoemission measurements along KX.

1. Introduction

The electronic structure in ferromagnetic Ni has been studied extensively over the last two decades by angle-resolved ultra-violet photoelectron spectroscopy (ARUPS) and band structure calculations. Among the ARUPS studies the most detailed are those by Eastman (1971, 1972), Heimann and Neddermeyer (1976, 1980), Petersson and Erlandsson (1978), Eastman *et al* (1978), Eberhardt and Plummer (1980), Heimann *et al* (1981), Raue *et al* (1983), Mårtensson and Nilsson (1984) and Sakisaka *et al* (1987a,b). Other photoemission studies of Ni, for example those involving x-ray photoelectron spectroscopy (XPS), have been reviewed by Davis (1986). From an early stage it was apparent that there were a number of serious discrepancies between the experimentally determined bands and those obtained from one-electron calculations. For instance, it was discovered—almost without exception (Smith *et al* 1977)—that the occupied d bandwidth was some 30 to 40% narrower than the results of band structure calculations (see, for example, Höchst *et al* 1977, Wang and Callaway 1974, 1977), and the measured ferromagnetic spin splitting was found to be about 40% of the calculated values (Dietz *et al* 1978, Heimann *et al* 1981). In addition, the width of photoemission peaks from Ni were found to be much broader than those from the

† Formerly at: School of Physics and Space Research, University of Birmingham, Birmingham B15 2TT, UK.

‡ Also formerly at: SERC Daresbury Laboratory, Warrington WA4 4AD, UK.

0953-8984/91/101337+14$03.50

corresponding transitions in Cu (Pendry and Hopkinson 1978). There was also the appearance of a satellite peak at 6 eV binding energy that resonates at a photon energy of 67 eV (Guillot *et al* 1977, Sakisaka *et al* 1987a,b).

The differences between the experimental and theoretical results for Ni outlined above stimulated a considerable amount of interest in the late 1970s and early 1980s. It was demonstrated that the discrepancies are due to intra-atomic correlation effects in the partially filled 3d band that are not included in conventional one-electron band structure calculations. Such behaviour can be conveniently described in terms of a complex self-energy that represents a generalized correction to the one-electron eigenvalues (Wendin 1981). The many different model treatments of the self-energy corrections developed during this period have been reviewed by Davis (1986). They include a t-matrix approach (assuming a low-density of d holes) by Liebsch (1979, 1981), a numerical solution to the Hubbard model for a finite system by Davis and Feldkamp (1979, 1980) and a perturbation method to second order in U/W, where U is the Coulomb integral in the Hubbard model and W the one-electron bandwidth, by Tréglia *et al* (1980, 1982); hereafter, referred to as the TDS model. All of these models appear to give a reasonable, semi-quantitative account of the experimental observations. More recently, Nolting *et al* (1989), using a generalized Hubbard model as a starting point, calculated an energy-exchange splittings near the X- and W-points and a Curie temperature in good agreement with experimental measurements (Borgiel *et al* 1989).

As we indicated earlier, it has been customary to use photoemission measurements to establish the validity of band structure calculations, see, for example, Himpsel (1983). However, because of the assumptions and limitations involved in making *direct comparisons increasing use has been made of realistic photocurrent* calculations based on a one-step model (Pendry 1976, see also Borstel and Thörner 1988 and references therein). Although the experience is that one-electron ground state potentials—calculated in most cases using the local (spin) density approximation (L(S)DA) in density functional theory—can provide a useful description of the photoemission from a variety of metals and alloys, more detailed comparisons between experiment and theory demand an improved approach. *Photoemission probes the excited state and so* correlation effects are always present; they are significant even for the nearly free electron metals Na, Mg, Al and Be, since the measured valence bandwidths are somewhat smaller, and the gaps somewhat larger, than values given by one-electron (LDA) eigenvalues (Jensen and Plummer 1985, Plummer 1985, Lyo and Plummer 1988). Other examples where there are serious discrepancies include semi-conductors, for which the measured band gaps are considerably greater than those calculated (Godby *et al* 1987, Hybertsen and Louie 1987 and references therein), and, as indicated above, Ni. (It should be pointed out that there has been a good deal of success in establishing a first-principles description of self-energy effects in weakly scattering systems (Godby *et al* 1987, Hybertsen and Louie 1987, Northrup *et al* 1989). In contrast much less has been achieved in the case of the 3d transition metals, apart from the several model descriptions outlined above.) One requires, therefore, a calculational scheme for the photocurrent in which the presence of the surface, the electron–photon matrix elements and the many-body correlation effects *etc.* are all included. Formally, this is a difficult task since, in general, the self-energy operator is complex, non-local, spin- and energy-dependent. Nevertheless, there has been some progress as we indicate below.

There have been a number of previous attempts to include correlation effects in photocurrent calculations. Pendry and Hopkinson (1978) considered the difference

in the photoemission from Cu and Ni and demonstrated that correlation effects can have a significant effect on spectroscopic measurements. They showed that the inclusion of an energy-dependent lifetime for the hole in photocurrent calculations of Ni leads to an apparent narrowing of the one-electron d bandwidth. Nilsson and Larsson (1983) obtained improved agreement between photocurrent calculations and experimental data from Cu when they included self-energy corrections for the hole and electron, calculated for a homogeneous electron gas. Clauberg (1983) calculated the spin-resolved photocurrent from Ni(110) at a photon energy of 16.85 eV, which corresponds to emission from the $S_4^{\uparrow\downarrow}$ bands close to the X-point. He used the self-energy expression developed by Liebsch (1979, 1981) that was fitted to the experimental binding energies of the $X_2^{\uparrow\downarrow}$ states and the peak widths from Raue *et al* (1983). Very recently, Nolting *et al* (1990) calculated the photoemission from Ni above and below the Curie temperature, using an energy-, spin- and temperature-dependent self-energy developed by Nolting *et al* (1989), and they achieved good agreement with some previous photoemission and inverse photoemission spectra. However, despite the often highly satisfactory agreement obtained between experimental and calculated spectra, it should be noted that a relative weakness of each of these calculations on Ni—apart from those by Pendry and Hopkinson (1978), in which the real part of the self-energy was neglected—was the use of energy- and spin-independent imaginary parts of the self-energy. In addition, in none of the investigations were the calculations carried out over a *range* of photon energies. As a result the extent of the validity (or limitations) of the various models in $(E, \boldsymbol{k})$-space has not been properly examined.

In a recent paper (Jordan and Hoyland 1989) we compared the ARUPS measurements of Heimann *et al* (1981) from Ni(110) over the photon energy range from 11–18 eV with one-electron photocurrent calculations that were renormalized using the TDS self-energy. This approach appeared to account well for the dispersion of the initial states along the K(S)X direction, but it was apparent that the relative lifetimes of holes in the majority- and minority-spin bands are not described correctly by the TDS model. These observations were later confirmed by calculations of the photocurrent and the quasiparticle band structure along the ΓKX direction (Jordan 1989). In this present paper we describe a series of ARUPS measurements we have made on Ni(110) at photon energies from 20–45 eV. The measurements were carried out at a somewhat higher resolution than those reported earlier by Sakisaka *et al* (1987a,b) and they provide us with the opportunity to extend our investigations of the electronic structure and self-energy effects in Ni. Accordingly, we calculate the corresponding photocurrents using a one-step model with a potential for the excited state that includes self-energy corrections from TDS. It is important to note that we use the full energy- and spin-dependence of the imaginary part from the model in the calculations. Our aim is to investigate the magnitude and the E and $\boldsymbol{k}$ variation of self-energy effects in Ni by comparing the calculations with our experimental spectra and other previous photoemission data. In addition, we show that it may not always be appropriate to simply equate the differences between photoemission peaks positions and one-electron eigenvalues with the real part of the self-energy, as has often been the custom. We do not claim that the TDS model is superior to the other schemes, indeed, we recognize that there have been some questions concerning the approximations within the model (e.g., Taranko *et al* 1988). However, it has been shown previously that it does provide a reasonable description of the self-energy effects in Ni, and it has the obvious merits that it is readily calculable and can be included in photocurrent calculations in

straightforward manner. Furthermore, the real and imaginary parts have the correct analytical properties.

2. Experimental considerations

The photoemission measurements were performed using the VG ADES400 spectrometer on beam-line 6.2 (TGM) at the SRS, Daresbury Laboratory, UK. The surface of the Ni(110) specimen was cleaned *in situ* by successive cycles of Ar^+ bombardment and annealing at 600 °C (Hoyland 1989). The surface crystallography and cleanliness were monitored using the standard techniques of low energy electron diffraction and Auger electron spectroscopy. The operating pressure in the spectrometer chamber was $\sim 1 \times 10^{-10}$ mbar.

We carried out a series of measurements at normal emission over the photon energy range 20–45 eV using p-polarized light. The overall energy resolution was fixed at 0.14 eV with an angular resolution of ±2°. Several separate sets of measurements were performed using different geometrical arrangements in order to probe initial states of $\Sigma_1(S_1)$, $\Sigma_3(S_3)$ and $\Sigma_4(S_4)$ symmetries (Hermanson 1977). In the first set, $\Sigma_4(S_4)$ and $\Sigma_1(S_1)$ states were probed by setting the light polarization vector, $\boldsymbol{A}$, in the (001) plane; increasing the angle of incidence, ϕ, increases the coupling to states with $\Sigma_1(S_1)$ character. In the second set, $\boldsymbol{A}$ was in the $(1\bar{1}0)$ plane so that initial states of $\Sigma_3(S_3)$ and $\Sigma_1(S_1)$ were probed. As before an increase in ϕ increases the contribution of the $\Sigma_1(S_1)$ components in the spectra.

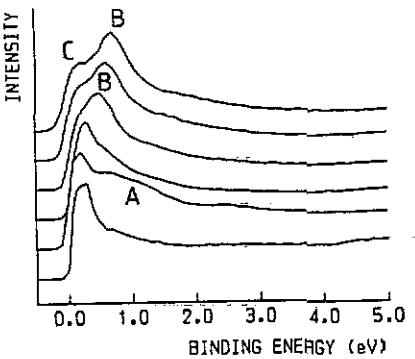

Figure 1. Photoemission spectra at normal emission from the (110) face of Ni. The photon energy increases in increments of 5 eV from 20 eV (bottom) to 45 eV (top). The angle of incidence is 30° from the normal in the (001) plane with p-polarization.

3. Results and preliminary interpretation

In figure 1 we show a typical set of spectra, as a function of the photon energy, with the light incident at an angle of $\phi = 30°$ and $\boldsymbol{A}$ in the (001) plane. Apart from a broad feature at ~ 1 eV (labelled A) in the spectrum at a photon energy of 25 eV, the spectra are characterised by a large peak (labelled B) that disperses away from

the Fermi level with increasing photon energy, i.e., from 0.2 eV at 20 eV to 0.9 eV at 45 eV. At a photon energy of 20 eV the spin splitting is just observable. The actual spin splitting was determined by fitting two Lorentzians of equal area and a step-like electron loss function for the secondary electron background to the experimental data. The peak positions (FWHM) for the minority- and majority-spin features were found to be 0.08 eV (0.23 eV) and 0.25 eV (0.27 eV), respectively. Assuming that the final states are free-electron-like, the two peaks correspond to emission from the $S_4^{\uparrow\downarrow}$ bands close to the X-point. These states are of e_g symmetry and our measured spin splitting of 0.17 eV is in agreement with the values of 0.20 eV and 0.18 eV reported by Heimann *et al* (1981) and Raue *et al* (1983), respectively. As the photon energy increases above 40 eV a shoulder (C) appears on the low binding energy side of B, between E_F and 0.5 eV. On studying the relative intensities of B and C as ϕ is increased, we conclude that they arise from initial states of $\Sigma_4(S_4)$ and $\Sigma_1(S_1)$ symmetries, respectively. In order to compare these data with other measurements we followed the usual practice and mapped the 'experimental' dispersion of the initial states $(\varepsilon_i, \boldsymbol{k}_i)$ by assuming a direct transition model and a free electron final state band with

$$\varepsilon_i = \varepsilon_f - h\nu$$

and

$$|\boldsymbol{k}_i| = \sqrt{\frac{2m(\varepsilon_f - V_0)}{\hbar^2}} - |\boldsymbol{G}|.$$

Here ν is the photon energy, ε_f is the energy of the photoelectron, $\boldsymbol{G}$ is a reciprocal lattice vector and V_0 is the inner potential. We find that with $V_0 = 10$ eV our resulting band structure is in good agreement with that published by Sakisaka *et al* (1987a,b).

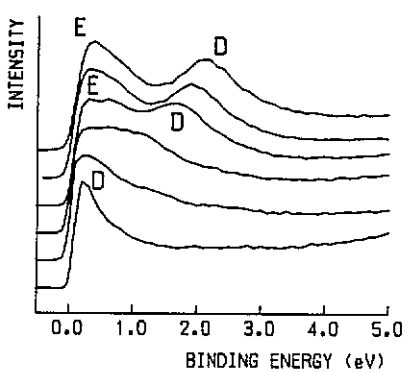

Figure 2. The conditions are the same as in figure 1 except that the light is incident in the $(1\bar{1}0)$ plane.

In figure 2 we show a typical set of spectra, as a function of the photon energy, with the light incident at angle of $\phi = 30°$ and $\boldsymbol{A}$ in the $(1\bar{1}0)$ plane. At the lower photon energies the spectra are characterised by a single peak (D) close to the Fermi level. At a photon energy of 30 eV the peak is substantially broader with contributions from four initial states (on the $S_3^{\uparrow\downarrow}$ and $S_1^{\uparrow\downarrow}$ bands). At higher photon energies two distinct

features (labelled D and E) appear, one that remains roughly stationary at a binding energy of ~ 0.3 eV whilst the other rapidly disperses away to 2 eV binding energy at a photon energy of 45 eV. On increasing ϕ it is apparent that the rapidly dispersing feature (D) is due to the emission from initial states of $\Sigma_3(S_3)$ symmetry whereas peak E arises from the emission from initial states of $\Sigma_1(S_1)$ symmetry. Using the scheme outlined in the previous paragraph we mapped the dispersion of the initial states (of $\Sigma_3(S_3)$ and $\Sigma_1(S_1)$ symmetries) and found good agreement with the semi-empirical band structure of Weling and Callaway (1982).

We have already made a preliminary analysis of the spectra shown in figures 1 and 2 on the basis of comparisons with a spin-polarized, one-electron band structure calculation (Jordan *et al* 1990). In common with previous studies we find that the main features in photoemission spectra may be described qualitatively in terms of a one-electron band picture with substantial self-energy corrections. In the following sections we describe a series of photocurrent calculations we have made for the Ni(110) surface using a one-step model that includes self-energy effects.

4. The calculation scheme

We carried out a series of photocurrent calculations using the scheme described previously by Jordan (1989) that includes self-energy corrections based on the TDS model. The latter can be readily included in photocurrent calculations since it is local and only spin- and energy-dependent, i.e., it is of the form $\Sigma_\sigma(E)$. The model is of a single band nature and so we make comparisons with experiment for bands of $\Sigma_4(S_4)$ and $\Sigma_3(S_3)$ symmetries individually and separately. A modified form of the (non-relativistic) NEWPOOL code (Hopkinson *et al* 1980, Larsson 1985) is used in which the spin- and angle-resolved elastic photocurrent is calculated by layer KKR multiple scattering techniques for a semi-infinite array of non-overlapping muffin-tin potentials. The presence of the surface is modelled by a step function that is in contact with the outermost layer of muffin-tins. The self-energy corrections are introduced by renormalizing separately the (single-particle) Green function propagators for the low- and high-energy states; the vertex corrections are assumed to have no substantial effect on the elastic part of the photocurrent (Almbladh 1985). An excitation potential is introduced for the photohole, therefore, of the form

$$V_\sigma(r,E) = \begin{cases} V_\sigma^0(r) + \Sigma_\sigma(E) & r \le r_{\mathrm{MT}} \\ \mathrm{i}V_{0\mathrm{i}}(E) & r > r_{\mathrm{MT}} \end{cases}$$

where $V_\sigma^0(r)$ is the ground state potential for spin σ, with eigenvalues $\varepsilon_{\mu\sigma}(k)$ (μ is the band index), r_{MT} is the muffin-tin radius and $\Sigma_\sigma(E)$ is the given by

$$\Sigma_\sigma(E) = U^2(\Delta_\sigma^0 + \Delta_\sigma(E) + \mathrm{i}\Gamma_\sigma(E)). \tag{1}$$

Here U is the intra-atomic Coulomb integral, Δ_σ^0 is a correction term, and $\Delta_\sigma(E)$ and $\Gamma_\sigma(E)$ are the real and imaginary parts of the self-energy given by TDS. These expressions can be included in the NEWPOOL code to allow the calculation of the photocurrent in the presence of self-energy corrections in the $l = 2$ angular momentum channel.

The ground state potentials were obtained from calculations using the spin-polarized, self-consistent-field, linear muffin-tin orbital (SCF-LMTO) method and the

Table 1. A comparison of the energies (in eV), with respect to the Fermi energy, of various critical points along the ΓKX direction determined using the NEWPOOL code with those of Moruzzi *et al* (1978) (MJW) and Wang and Callaway (1977) (WC).

Symmetry point	NEWPOOL	MJW	WC
$\Gamma_{12}^{\uparrow}$	−1.26	−1.35	−1.12
$\Gamma_{12}^{\downarrow}$	−0.60	−0.69	−0.65
$\Gamma_{25'}^{\uparrow}$	−2.24	−2.43	−2.31
$\Gamma_{25'}^{\downarrow}$	−1.54	−1.84	−1.77
$X_2^{\uparrow}$	−0.59	−0.59	−0.47
$X_2^{\downarrow}$	+0.10	+0.10	+0.11
$X_5^{\uparrow}$	−0.32	−0.33	−0.30
$X_5^{\downarrow}$	+0.35	+0.37	+0.33

Table 2. A comparison of the energies (in eV), with respect to the Fermi energy, of some high energy critical points along the ΓKX direction determined using the NEWPOOL code with those of Papaconstantopoulos (1986) (Papa) and Szmulewicz and Pease (1978) (SP).

Symmetry point	NEWPOOL	Papa	SP
X_1	9.33	9.15	9.28
$X_{5'}$	14.66	14.90	14.71
X_3	19.49	20.00	19.89
X_1	22.76	23.28	23.15
Γ_{15}	26.49	27.24	27.17
$\Gamma_{25'}$	30.27	30.34	30.29

LSDA. The corresponding densities of d states (Guo 1989) were used in the expressions for $\Delta_\sigma(E)$ and $\Gamma_\sigma(E)$ given by TDS. Since the potentials were obtained from calculations involving the LSDA a correction term, Δ_σ^0, appears in equation (1) to take into account the correlations already included (Tréglia *et al* 1982, Clauberg 1983). However, the real and imaginary parts of the self-energy are related by a Hilbert transformation and so Δ_σ^0 is independent of energy. By using an option in the NEWPOOL code we calculated the ground state energy bands, $\varepsilon_{\mu\sigma}(\boldsymbol{k})$; they are shown along the ΓKX direction in Jordan *et al* (1990) and so are not reproduced here. In tables 1 and 2 we compare the energies of various critical points so determined with the corresponding values obtained from other one-electron calculations. Not surprisingly, the agreement is generally very good both below and above the Fermi level.

We show in figure 3 the spin-resolved real and imaginary parts of the self-energy from equation (1), with $\Delta_\sigma^0 = 0$. They are similar to those published by TDS for a rectangular density of states, although additional detail is evident in our plots due to our use of a more realistic and structured density of d states. TDS discussed in some detail the implications of the energy dependence of the real and imaginary parts, which we will not re-iterate here. The quasiparticle bands of $\Sigma_3(S_3)$ and $\Sigma_4(S_4)$ symmetries are given by the loci in $(E, \boldsymbol{k})$-space of the maxima in the spectral function

$$\tilde{A}_{\mu\sigma}(\boldsymbol{k}, E) = -\frac{1}{\pi} \operatorname{Im} m(E - \varepsilon_{\mu\sigma}(\boldsymbol{k}) - \Sigma_\sigma(E))^{-1} \tag{2}$$

where $\varepsilon_{\mu\sigma}(\boldsymbol{k})$ are the one-electron (ground state) eigenvalues for band μ ($\equiv \Sigma_3(S_3)$ or

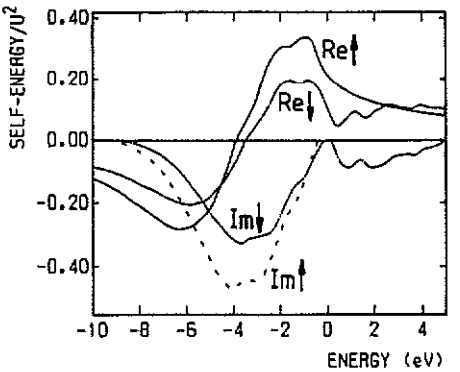

Figure 3. The spin-dependent, real and imaginary parts of the self-energy for Ni calculated using the TDS model.

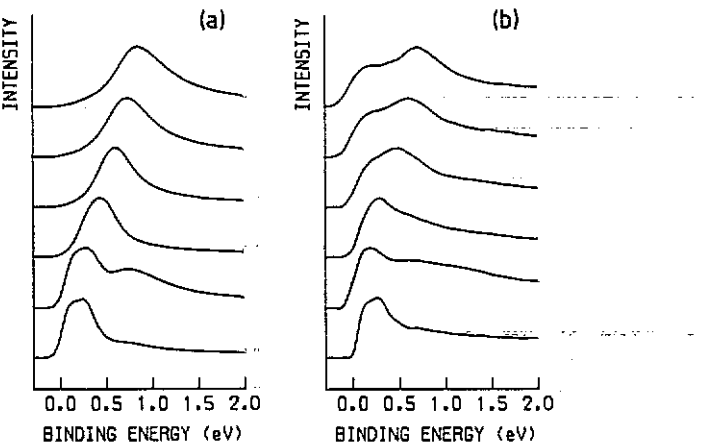

Figure 4. A comparison of (*a*) photocurrent calculations including self-energy corrections for Σ_4 initial states with (*b*) experimental angle-resolved photoemission measurements of Ni(110) for Σ_4 and Σ_1 initial states. The photon energy increases in increments of 5 eV from 20 eV (bottom) to 45 eV (top).

$\Sigma_4(S_4)$) and spin σ, with $\Sigma_\sigma(E)$ from equation (1).

5. Comparison of the data with calculations

In figure 4(*a*) we show the calculated photocurrents for the bands of $\Sigma_4(S_4)$ symmetry only from the Ni(110) surface, using the approach described above. The spin-resolved components of the photocurrents were calculated individually, summed and convoluted with a step function at E_F and a Lorentzian with a FWHM = 0.15 eV to simulate the experimental conditions. We took particular care to ensure that a sufficiently large set of reciprocal lattice vectors was used in the plane-wave expansion in the NEWPOOL code; we found that 65 were required in order to obtain convergence. For the initial states, $V_{0i}(E)$ was set to a small, constant (negative) value. For the high energy states we used an energy-dependent, parameterized expression for $V_{0i}(E)$ that was obtained from the 'characteristic' mean-free path curve (Brundle 1975), and fitted to

the lifetimes determined by Heimann *et al* (1981) from their low energy photoemission data.

We chose values for the parameters U (1.8 eV), $\Delta_{\uparrow}^{0}$ (-0.126 eV^{-1}) and $\Delta_{\downarrow}^{0}$ ($-0.149\ eV^{-1}$) that gave the best fit with the measured values of the binding energies of the $X_2^{\uparrow\downarrow}$ states (Heimann *et al.* 1981, Raue *et al.* 1983). A comparison with figures 1 and 4(b) indicates that excellent agreement can be achieved with the experimental spectra. (It is important to note that the spectra shown in figures 1 and 4(b) contain features derived from initial states of $\Sigma_1(S_1)$ symmetry. However, the calculations have only been made for states with $\Sigma_4(S_4)$ symmetry, in accordance with the spirit of the TDS model.) At a photon energy of 20 eV states close to the X-point are being probed. As the photon energy increases the dispersion of the peak in figure 4(a) closely matches that in figure 4(b). It is also clear that this feature broadens considerably as it moves away from E_F, (and away from the X-point), and there is very good agreement between the calculated and the experimentally observed widths. This broadening is due to the rapid increase in $|\Gamma_\sigma(E)|$ below E_F, as shown in figure 3. As a result, at photon energies of 30 eV and above, the exchange splitting is not resolvable in either the calculated or experimental spectra. We note that the broad peak (A) at $\sim$ 1 eV seen in the experimental spectra at a photon energy of 25 eV is reproduced both in position and width in the theoretical spectra; we comment on this origin of this feature below.

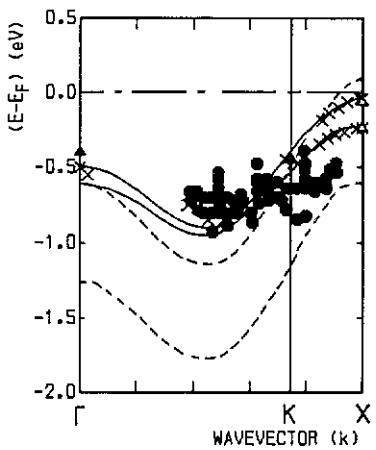

Figure 5. Comparisons of the calculated and experimentally determined dispersion for states of $\Sigma_4(S_4)$ symmetry along the ΓKX direction. – – –, band calculations using ground state potentials; ——, loci of the maxima in the quasiparticle spectral functions. ●, Sakisaka *et al* (1987); ×, Heimann *et al* (1981) and Himpsel (1989); ▲, Eberhardt and Plummer (1980); Δ, Raue *et al* (1983).

In figure 5 we have plotted the loci of the maxima in the spectral function, obtained from equations (1) and (2), for the $\Sigma_4(S_4)$ bands. Also shown are the ground state energy bands and the results from a number of previous experimental studies. It is clear that our quasiparticle band structure shows substantially improved agreement with the experimental data than the ground state bands, right along the ΓKX direction. It is interesting to note that in contrast to the approximately rigid shift obtained in the one-electron (LSDA) calculations, the exchange splitting becomes rather strongly energy-dependent when self-energy effects are included (see also Borgiel *et*

al 1989 and Nolting *et al* 1989). Indeed, it varies from ~ 0.18 eV at the X-point to < 0.10 eV at the bottom of the band. Unfortunately, because of the concomitant rapid increase in $|\Gamma_\sigma(E)|$ below E_F it is not possible to delineate such behaviour in the spin-integrated photoemission measurements except between the X- and K-points where, as has already been noted (Jordan 1989), there is good agreement between the calculations and the experimental data of Heimann *et al* (1981) and Himpsel (1989). We identify the broad peak (A) at ~ 1 eV in the experimental and theoretical spectra at a photon energy of 25 eV, see figures 1 and 4, with emission from the bottom of the Σ_4 band, where there is a high density of initial states. These states can couple into an unoccupied final state band due to the large lifetime broadening.

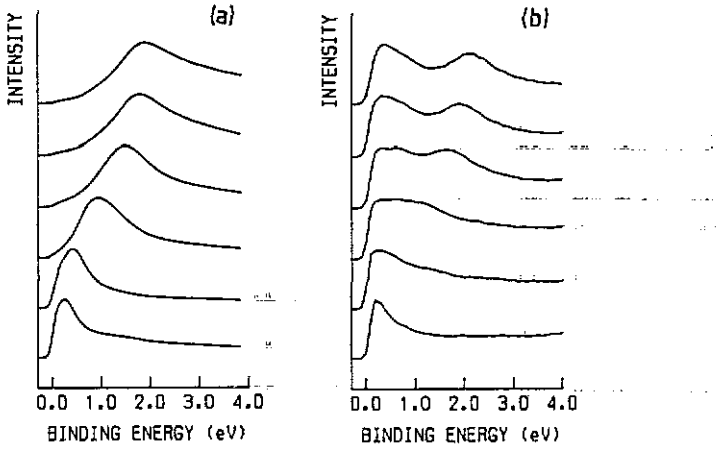

Figure 6. A comparison of (*a*) photocurrent calculations including self-energy corrections for Σ_3 initial states with (*b*) experimental angle-resolved photoemission measurements of Ni(110) for Σ_3 and Σ_1 initial states. The photon energy increases in increments of 5 eV from 20 eV (bottom) to 45 eV (top).

In figure 6(*a*) we show the calculated photocurrents over a range of photon energy from states of $\Sigma_3(S_3)$ symmetry using $U = 1.8$ eV, $\Delta^0_\uparrow = -0.16$ eV^{-1} and $\Delta^0_\downarrow = -0.10$ eV^{-1}. These values of Δ^0_σ are slightly different from those for the $\Sigma_4(S_4)$ bands; they were chosen to fit the Fermi surface data, the photoemission and inverse photoemission results reported by Heimann *et al* (1981), Raue *et al* (1983) and Donath *et al.* (1990), and references therein, for the the position where the minority-spin band crosses the Fermi level and the binding energies of the $X_5^{\uparrow\downarrow}$ states. At a photon energy of 20 eV the peak just below E_F corresponds to emission from $X_5^\uparrow$ states. We note that the dispersion of peak D in figure 2 is reproduced well in the calculations. As was noted for the other geometry the features broaden considerably as they move away from E_F and the calculated widths are in very good agreement with those observed.

In figure 7 we have plotted the ground state $\Sigma_3(S_3)$ energy bands, the loci of the maxima in the corresponding quasiparticle spectral function, obtained from equations (1) and (2), together with several sets of experimentally determined points. Again, we see that the inclusion of the self-energy corrections leads to a much improved agreement between experiment and theory. The sharp reduction of the spin splitting between the quasiparticle bands near the K-point is a consequence of structure in the (real part of the) self-energy corrections at that energy, see figure 3. In fact, small changes to

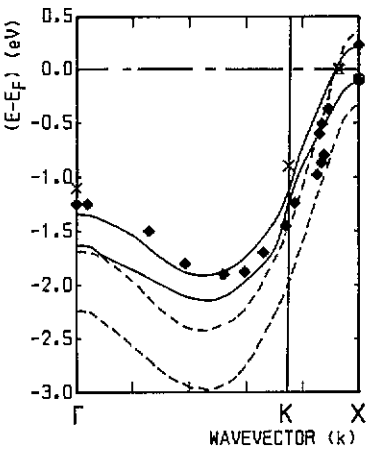

Figure 7. Comparisons of the calculated and experimentally determined dispersion for states of $\Sigma_3(S_3)$ symmetry along the ΓKX direction. – – –, band calculations using ground state potentials. ——, loci of the maxima in the quasiparticle spectral functions. ⧖, de Haas–van Alphen data; ♦, Heimann *et al* (1981) and Himpsel (1989); ×, Eberhardt and Plummer (1980); ●, Raue *et al* (1983).

the values of Δ_σ^0, although making only minor differences to the calculated spectra, can actually result in an *inverse* exchange splitting in this region. The possibility of similar behaviour was suggested also by Borgieł *et al* (1989) and Nolting *et al* (1989) in the uppermost d subband.

In table 3 we compare the calculated critical points from the quasiparticle bands with various experimental data from photoemission measurements. Overall we obtain good agreement. It should be noted that it has often been the practice to equate differences between the peak positions in photoemission spectra and the ground state eigenvalues with the real part of the self-energy. However, figure 3 shows that the imaginary part of the self-energy, $\Gamma_\sigma(E)$, is strongly energy dependent and so it must also play a role in determining the energy position of maxima in the spectral function, equation (2). As the results in table 3 show, in the case of the $\Sigma_4(S_4)$ bands the differences between using (*a*) the full self-energy and (*b*) the real part only are small at the critical points Γ_{12}, K_4 and X_2, although at the bottom of the band (near $k \sim 0.5$) the discrepancy amounts to 0.13 eV. In the case of the $\Sigma_3(S_3)$ bands, larger differences are apparent at $\Gamma_{25'}$ and K_3, and at the bottom of the band, the discrepancy is ~ 0.8 eV!

Starnberg and Nilsson (1988) determined the real part of the self-energy for Ni by analysing previous photoemission data. They decoupled the sp and d bands but did not discriminate between the different spins or the d-band symmetries. Although there is some scatter in their data, they found a linear relationship with energy for the d-band contribution, namely

$$\Delta' \simeq -0.44(E - E_F).$$

In figure 8, therefore, we compare the energy dependences of our spin-resolved TDS self-energies for the $\Sigma_3(S_3)$ and $\Sigma_4(S_4)$ bands with a line of slope -0.44 and we see that they are in very good accord.

Table 3. A comparison of experimentally determined critical point energies (in eV), with respect to the Fermi energy, with those determined in this study using the full self-energy correction (i.e., including the real and imaginary parts) and the real part only. $\langle\cdots\rangle$ denotes values that are the average of the two spins.

Symmetry point	Experimental	Full self-energy	Real part only
$\Gamma_{12}^{\uparrow}$	$\langle -0.40\rangle$ [a]	−0.60	−0.63
$\Gamma_{12}^{\downarrow}$	$\langle -0.5\rangle$ [b]	−0.48	−0.50
$K_4^{\uparrow}$	$\langle -0.45\rangle$ [a]	−0.52	−0.53
$K_4^{\downarrow}$		−0.39	−0.40
$X_2^{\uparrow}$	−0.24 [c], −0.24 [d]	−0.22	−0.22
$X_2^{\downarrow}$	−0.06 [c], −0.04 [d]	−0.03	−0.03
$\Gamma_{25'}^{\uparrow}$	$\langle -1.25\rangle$ [b]	−1.63	−1.76
$\Gamma_{25'}^{\downarrow}$	$\langle -1.10\rangle$ [a]	−1.34	−1.40
$K_3^{\uparrow}$	$\langle -0.90\rangle$ [a]	−1.24	−1.48
$K_3^{\downarrow}$		−1.12	−1.18
$X_5^{\uparrow}$	−0.10 [c], −0.11 [d]	−0.11	−0.11
$X_5^{\downarrow}$	+0.23 [d]	+0.23	+0.23

[a] Eberhardt and Plummer (1980).
[b] Himpsel (1989).
[c] Raue *et al* (1983).
[d] Heimann *et al* (1981).

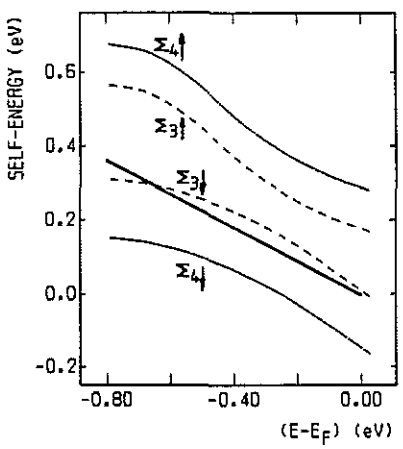

Figure 8. Comparison of the TDS self-energy and that determined experimentally for pure d bands (Starnberg and Nilsson 1988). The heavy full has a gradient of −0.44 (see text).

6. Concluding remarks

We have shown that when correlation effects are included in realistic photocurrent calculations for Ni(110), good agreement can be achieved with angle-resolved, spin-integrated UV photoemission measurements over a range of photon energies. Using

the local model of Tréglia *et al* (1982) for the self-energy corrections to one-electron eigenvalues, we can reproduce the dispersion of the quasiparticle states of $\Sigma_3(S_3)$ and $\Sigma_4(S_4)$ symmetry along the $\Gamma(\Sigma)K(S)X$ direction. The degree of agreement we find between our calculations and experimental data gives further support to the view from earlier studies that, at least for the d bands, the self-energy is essentially only energy dependent (see, for example, Eberhardt and Plummer 1980, Davis 1986, Starnberg and Nilsson 1988); an assumption that underlies the present analysis. We find that the correlations produce a marked energy dependence of the spin splitting along the ΓKX direction, indeed, it is conceivable that an inverse exchange splitting may occur at certain values of k. We have shown previously (Jordan and Hoyland 1989) that just below E_F the relative lifetimes of holes in the minority- and majority-spin bands are not correctly predicted by the TDS model. Although the calculated widths of the minority-spin features are in good agreement with the published data the widths of the majority-spin features are consistently too small (Jordan 1989). Nevertheless, the imaginary part of the self-energy calculated at the bottom of the d band (~ 1.6 eV) is in good agreement with the peak widths ($\sim 2\Gamma$) measured by Eberhardt and Plummer (1980). We have shown also that significant errors may arise in experimental determinations of self-energy corrections if the differences between photoemission peak positions and one-electron eigenvalues are equated simply with the *real* part of the self-energy.

We should point out that the TDS model is not necessarily superior to other models—for example, those mentioned in the introduction—since they all appear to give quantitatively similar results for Ni (Davis 1986). However, we have shown that despite its apparent inadequacies the TDS model provides a surprisingly good description of the self-energy corrections in Ni, at least for the $\Sigma_3(S_3)$ and $\Sigma_4(S_4)$ bands. We anticipate that spin-resolved photoemission measurements will soon be available. They will undoubtedly provide the detailed quantitative information necessary for the development of improved descriptions of the correlation effects in Ni.

Acknowledgments

This work was funded by an Award from the Science and Engineering Research Council, UK and we are grateful for their support. We wish to acknowledge the help and assistance of the support staff on beam-line 6.2 and the SRS machine crews at the Daresbury Laboratory. We also thank Dr. E Seddon for helping with some of the data collection, Drs F J Himpsel and Y Sakisaka for providing additional experimental data, and Dr P J Durham for many useful discussions. MAH thanks the School of Physics and Space Research, University of Birmingham for the provision of a Research Studentship.

References

Almbladh C-O 1985 *Phys. Scr.* **32** 341
Borgiel W, Nolting W and Donath M 1989 *Solid State Commun.* **72** 825
Borstel G and Thörner G 1988 *Surf. Sci. Rep.* **8** 1
Brundle C 1975 *Surf. Sci.* **48** 99
Clauberg R 1983 *Phys. Rev.* B **28** 2561
Davis L C 1986 *J. Appl. Phys.* **59** R25

Davis L C and Feldkamp L A 1979 *J. Appl. Phys.* **50** 1944
—— 1980 *Solid State Commun.* **34** 141
Dietz E, Gerhardt U and Maetz C J 1978 *Phys. Rev. Lett.* **40** 892
Donath M, Dose V, Ertl K and Kolac U 1990 *Phys. Rev.* B **41** 5509
Eastman D E 1971 *J. Physique* **32** 293
—— 1972 *Electron Spectroscopy* ed D A Shirley (Amsterdam: North-Holland) p 487
Eastman D E, Himpsel F J and Knapp J A 1978 *Phys. Rev. Lett.* **40** 1514
Eberhardt W and Plummer E W 1980 *Phys. Rev.* B **21** 3245
Godby R W, Schluter M and Sham L J 1987 *Phys. Rev.* B **35** 4170
Guillot C, Ballu Y, Paigne J, Leconte J, Jain K P, Thiry P, Pinchaux R, Petroff Y and Falicov L M 1977 *Phys. Rev. Lett.* **39** 1632
Guo G Y 1989 private communication
Heimann P and Neddermeyer H 1976 *J. Phys. F: Met. Phys.* **6** L257
—— 1980 *J. Magn. Magn. Mater.* **15–18** 1143
Heimann P, Himpsel F J and Eastman D E 1981 *Solid State Commun.* **39** 219
Hermanson J 1977 *Solid State Commun.* **22** 9
Himpsel F J 1983 *Adv. Phys.* **32** 1
Himpsel F J 1989 private communication
Höchst H, Hüfner S and Goldmann A 1977 *Z. Phys.* B **26** 133
Hopkinson J F L, Pendry J B and Titterington D J 1980 *Comput. Phys. Commun.* **19** 69
Hoyland M A 1989 *PhD Thesis* University of Birmingham, UK
Hybertsen M S and Louie S G 1987 *Comments Condens. Matter Phys.* **13** 223
Jensen E and Plummer E W 1985 *Phys. Rev. Lett.* **55** 1912
Jepsen D W, Himpsel F J and Eastman D 1982 *Phys. Rev.* B **26** 4039
Jordan R G 1989 *J. Phys.: Condens. Matter* **1** 9795
Jordan R G and Hoyland M A 1989 *Solid State Commun.* **72** 433
Jordan R G, Hoyland M A and Seddon E A 1990 *J. Phys.: Condens. Matter* **2** 779
Larsson C G 1985 *Surf. Sci.* **152/153** 213
Liebsch A 1979 *Phys. Rev. Lett.* **43** 1431
—— 1981 *Phys. Rev. B* **23** 5203
Lyo In-Whan and Plummer E W 1988 *Phys. Rev. Lett.* **60** 1558
Mårtensson H and Nilsson P O 1984 *Phys. Rev.* B **30** 3047
Moruzzi V L, Janak J F and Williams A R 1978 *Calculated Properties of Metals* (New York: Pergamon)
Nilsson P O and Larsson C G 1983 *Phys. Rev.* B **27** 6143
Nolting W, Borgiel W, Dose V and Fauster Th 1989 *Phys. Rev.* B **40** 5015
Nolting W, Braun J, Borstel G and Borgiel W 1990 *Phys. Scr.* **41** 601
Northrup J E, Hybertsen M S and Louie S G 1989 *Phys. Rev.* B **39** 8198
Papaconstantopoulos D A 1986 *Handbook of the Band Structure of Elemental Solids* (New York: Plenum)
Pendry J B 1976 *Surf. Sci.* **57** 679
Pendry J B and Hopkinson J F L 1978 *J. Phys. F: Met. Phys.* **8** 1009
Petersson L-C and Erlandsson R 1978 *Phys. Rev.* B **17** 3006
Plummer E W 1985 *Surf. Sci.* **152/153** 162
Plummer E W and Eberhardt W 1979 *Phys. Rev.* B **20** 1444
Raue R, Hopster H and Clauberg R 1983 *Phys. Rev. Lett.* **50** 1623
Sakisaka Y, Komeda T, Onchi M, Kato H, Masuda S and Yagi K 1987a *Phys. Rev. Lett.* **58** 733
—— 1987b *Phys. Rev.* B **36** 6383
Starnberg H I and Nilsson P O 1988 *J. Phys. F: Met. Phys.* **18** L247
Smith R J, Anderson J, Hermanson J and Lapeyre G J 1977 *Solid State Commun.* **21** 459
Szmulewicz F and Pease D M 1978 *Phys. Rev.* B **17** 3341
Taranko R, Taranko E and Malek J 1988 *J. Phys. F: Met. Phys.* **18** L87
Tréglia G, Ducastelle F and Spanjaard D J 1980 *J. Physique* **41** 281
—— 1982 *J. Physique* **43** 341
Wang C S and Callaway J 1974 *Phys. Rev.* B **9** 4897
—— 1977 *Phys. Rev.* B **15** 298
Weling F and Callaway J 1982 *Phys. Rev.* B **26** 710
Wendin G 1981 *Structure and Bonding* vol 45 (Berlin: Springer)